Available online at www.sciencedirect.com
SCIENCE DIRECT
Journal of Molecular Spectroscopy 237 (2006) 53–62
Journal of MOLECULAR SPECTROSCOPY
www.elsevier.com/locate/jms

Fourier transform absorption spectra of $H_2{}^{17}O$ and $H_2{}^{18}O$ in the 8000–9400 cm^{-1} spectral region

A.-W. Liu [a,b], S.-M. Hu [a,b,*], C. Camy-Peyret [c], J.-Y. Mandin [c], O. Naumenko [d], B. Voronin [e]

[a] *Hefei National Laboratory for Physical Sciences at the Microscale, University of Science and Technology of China, Hefei, 230026, China*
[b] *Shanghai Institute for Advanced Studies, University of Science and Technology of China, Shanghai, 201315, China*
[c] *Laboratoire de Physique Moléculaire pour l'Atmosphère et l'Astrophysique, CNRS and Université Pierre et Marie Curie, Boite 76, 4 Place Jussieu, 75252 Paris Cedex 05, France*
[d] *Institute of Atmospheric Optics, SB, Russian Academy of Sciences, Tomsk, Russia*
[e] *Department of Physics and Astronomy, University College London, London, WC1E 6BT, UK*

Received 28 January 2006; in revised form 10 February 2006
Available online 6 March 2006

Abstract

Fourier transform spectra of water vapor enriched in ^{18}O and ^{17}O were recorded between 8012 and 9336 cm^{-1} and analyzed for the first time. High accuracy ab initio predictions of line positions and intensities by Partridge and Schwenke [J. Chem. Phys. 106 (1997) 4618–4639; 113 (2000) 6592–6597] were used in the process of spectrum assignment. Transitions involving the (031), (111), (130), (210), and (012) upper vibrational states were identified in the recorded spectra. As a result, 514 and 244 precise ro-vibrational energy levels were derived for the $H_2{}^{18}O$ and $H_2{}^{17}O$ molecules, respectively. High-order resonance perturbations between levels of the vibrational states involved were evidenced leading to the identification of a number of rotational levels of the (050) and (060) highly excited bending states.

Keywords: Vibration–rotation spectroscopy; Water vapor absorption; Spectroscopic parameters

1. Introduction

The contribution of water vapor to the total absorption of solar radiation by the Earth atmosphere is very significant in several spectral intervals from the infrared (IR) to the visible. High-resolution absorption spectra for the main isotopic species $H_2{}^{16}O$ in the 8000–9600 cm^{-1} spectral region were studied in details [1–3]. The spectra of two minor isotopologues of the water molecule, $H_2{}^{18}O$ and $H_2{}^{17}O$, have been already analyzed both for the 2ν polyad (first hexad) [4,5] and for the 3ν polyad (first decade) [6,7]. Therefore it is desirable to extend these investigations in the 1 μm spectral region to complete the spectroscopic coverage in the near IR region. The present work is devoted to the analysis of Fourier transform (FT) spectra of $H_2{}^{18}O$ and $H_2{}^{17}O$ in the domain 8012–9336 cm^{-1}. This region corresponds to the second hexad of interacting vibrational states, i.e., the polyad {(050), (130), (031), (210), (111), and (012)} in the effective Hamiltonian and normal mode terminology. For the line assignment, the global variational calculations by Partridge and Schwenke [8,9] were used and found to be very accurate in the studied region.

In a recent paper [3], new spectroscopic line parameters for weak water vapor transitions in the 7400–9600 cm^{-1} region were published, which were retrieved from a long path-length FT spectrum [10]. Due to the high sensitivity provided by this experimental technique, 548 weak lines corresponding to $H_2{}^{18}O$ and $H_2{}^{17}O$ absorption lines observed in natural abundance water vapor were identified in the region under study.

* Corresponding author. Fax: +86 551 360 2969.
E-mail address: smhu@ustc.edu.cn (S.-M. Hu).

0022-2852/$ - see front matter © 2006 Elsevier Inc. All rights reserved.
doi:10.1016/j.jms.2006.02.008

However, as will be seen from the forthcoming analysis, FT spectra of the ^{17}O and ^{18}O-enriched water yielded considerably more experimental information on the vibrationally excited states of the two heavy isotopologues than in [3].

2. Experimental details

2.1. $H_2{}^{18}O$ spectrum, Hefei

The ^{18}O-enriched water sample was purchased from Aldrich Chemical Company, Inc. The stated isotopic concentration of ^{18}O is 95%. The absorption spectra were recorded with a Bruker IFS 120HR FT spectrometer equipped with a path-length adjustable multi-pass gas cell. The maximum optical path length is 105 m. We have recorded the spectra in different regions below 12 000 cm^{-1}. For the spectral region covered in this study, a tungsten source, a CaF_2 beam splitter and a Ge-diode detector were used for the measurements. The cell was operated at room temperature, stabilized by an air-conditioning system. The pressure was measured using two capacitance manometers of 200 Pa and 133 hPa full-scale range with an overall accuracy of 0.5%. In consideration of the wide spectral range and the large variation of absorption line intensities, several spectra were recorded with different sample pressure (215, 1307 Pa) and absorption path length (15, 105 m) at 0.015 cm^{-1} unapodized resolution. The line positions were calibrated with the $H_2{}^{16}O$ lines given by the HITRAN-2004 [12] database. The accuracy of the line positions of unblended and not too weak lines was estimated to be better than 0.0012 cm^{-1}. An overview of the spectrum in the region of 8000–9400 cm^{-1} is shown in Fig. 1.

2.2. $H_2{}^{17}O$, $H_2{}^{18}O$ spectrum, and kitt peak

The ^{18}O-enriched (73% ^{18}O, 27% ^{16}O), the ^{17}O-enriched (5% ^{17}O, 16% ^{18}O, and 79% ^{16}O) and the natural water vapor spectra in the 8500–9330 cm^{-1} spectral region were recorded using the FT interferometer of the National Solar Observatory (Kitt Peak, AZ). The experimental procedure and data reduction have been already outlined in [4,6]. By comparison of the spectra with different path lengths and isotopic abundances, 636 and 447 observed lines were assigned to $H_2{}^{18}O$ and $H_2{}^{17}O$ transitions, respectively.

3. Line assignments and line lists construction and validation

The line positions obtained from the spectra recorded with the two experimental setups were compared and coincided very well (0.0018 cm^{-1} absolute averaged deviation). Since the $H_2{}^{18}O$ spectra recorded in Hefei covered a larger spectral region and contained significantly more lines, they were mostly used for the derivation of the $H_2{}^{18}O$ energy levels. Similarly, as the $H_2{}^{17}O$ spectra were recorded at Kitt Peak with a higher ^{17}O isotopic abundance, they included more lines of the corresponding isotopologue and were preferred for the retrieval of the $H_2{}^{17}O$ energy levels. For identification purposes, relative experimental intensities were estimated for all spectral lines from peak absorption values (using the method proposed in [11]). These intensities were then scaled to theoretically calculated ones [9] for pure $H_2{}^{18}O$ and $H_2{}^{17}O$. The good agreement between the calculated and observed line intensities for both isotopic species is evident from Figs. 2 and 3 for the whole and selected regions, respectively.

With the help of the highly accurate theoretical calculations of [9] (SP in the following), all observed lines were

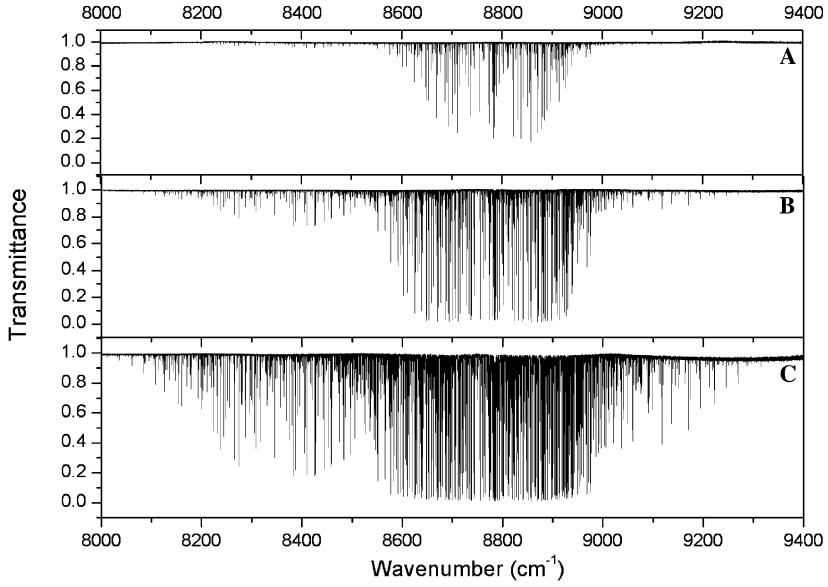

Fig. 1. Overview of the ^{18}O-enriched spectrum in the 8000–9400 cm^{-1} region. Experimental conditions: CaF_2 beam splitter, Ge detector, (A) 215 Pa, 15 m; (B) 1307 Pa, 15 m; (C) 1307 Pa, 105 m.

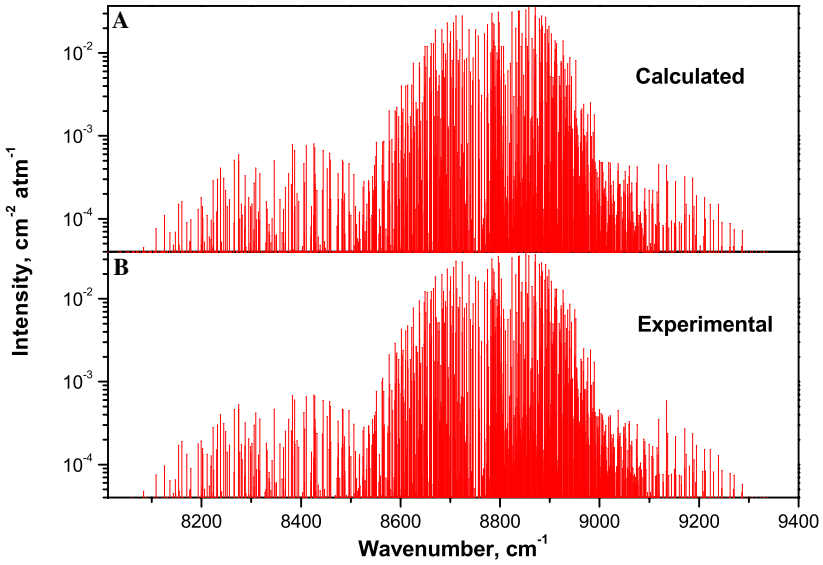

Fig. 2. Comparison of the pure $H_2{}^{17}O$ and $H_2{}^{18}O$ stick spectrum (at 296 K) in the whole 8012–9336 cm^{-1} region: (A) calculation by Schwenke and Partridge [8,9]; (B) experimental data derived from this work. Only assigned lines were used in both panels.

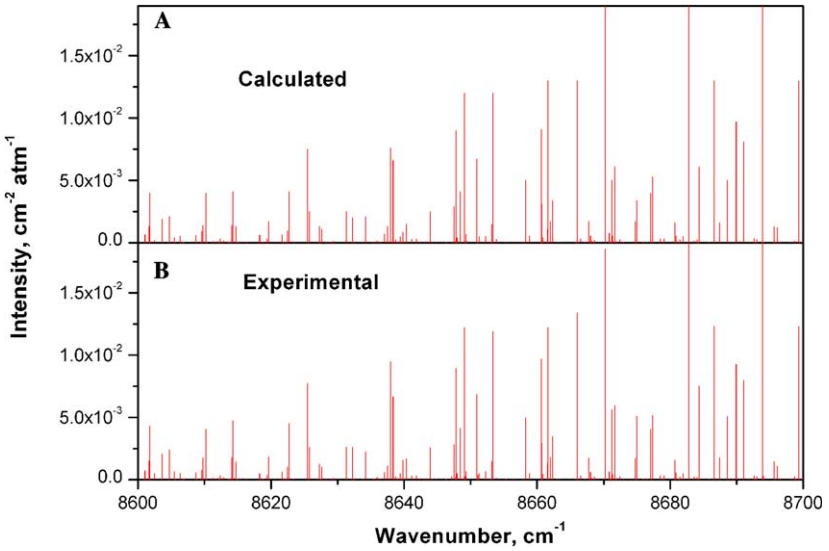

Fig. 3. Comparison of the pure $H_2{}^{17}O$ and $H_2{}^{18}O$ stick spectrum (at 296 K) in the selected 8600–8700 cm^{-1} region: (A) calculation by Schwenke and Partridge [8,9]; (B) experimental data derived from this work. Only assigned lines were used in both panels.

assigned in a straightforward manner. A summary of the derived spectroscopic information is given in Table 1 in comparison with the data published in [3]. The final $H_2{}^{18}O$ and $H_2{}^{17}O$ identification lists are attached to the paper as Supplementary data. The lists contain 1567 and 447 absorption lines, which correspond to 1696 and 467 transitions of $H_2{}^{18}O$ and $H_2{}^{18}O$, respectively, when accounting for multiple or blended lines. For each line, the experimental and calculated (SP) intensities are provided with the ro-vibrational assignment. Lines superimposed on $H_2{}^{16}O$ or on other isotopic lines are marked. A few relatively strong lines of both ^{18}O and ^{17}O isotopologues were unrecoverable because of blends and are then absent from the line lists.

We compared our results both with the HITRAN-2004 database [12] and with [3] in the whole considered spectral range. Fig. 4 shows a comparison between the stick spectra for the pure $H_2{}^{18}O$ and $H_2{}^{17}O$ species in the region 9000–9200 cm^{-1} for three data sources: HITRAN-2004, [3] and the present work. It is obvious that our new line lists contains many more weak absorption lines than [3]. It turns out that, for common lines, our positions and intensities match very well with those of [3]: the positions agree within 0.0025 cm^{-1} (absolute averaged deviation), while the average intensity ratio of our data to [3] is 0.96. This comparison is demonstrating, in fact, that the SP intensity calculation [9] used for scaling our data is of reasonably high accuracy. It is worth to note here that the first

Table 1
Summary of derived spectroscopic information

$(v_1v_2v_3)$	$H_2{}^{17}O$						$H_2{}^{18}O$					
	Vibrational energy (cm^{-1})		No. of levels		Δ_1	Δ_2	Vibrational energy (cm^{-1})		No. of levels		Δ_1	Δ_2
	Calc.	Obs.	Obs.	[3]			Calc.	Obs.	Obs.	[3]		
(050)	7527.62		1		0.06	0.06	7514.28		4		0.15	0.15
(130)	8260.85		5		0.02	0.06	8249.07	8249.035	76	12	0.04	0.19
(031)	8356.58	8356.531	26	12	−0.07	−0.13	8341.11	8341.107	116	51	−0.02	−0.09
(210)	8749.99	8749.91*	40	4	−0.07	−0.10	8739.59	8739.525	85	24	−0.04	−0.08
(111)	8792.59	8792.544	113	68	−0.03	−0.06	8779.73	8779.719	143	99	0.03	−0.18
(060)	8853.92		1		−0.14	−0.14	8838.98		1		−0.11	−0.11
(012)	8982.85	8982.869	60		0.02	0.04	8967.49	8967.565	88	34	0.08	0.13
		Total	244	84				Total	514	220		
		New	164					New	298			

Obs., observed in this work; Calc., calculated in [8]; Δ_1, average Obs.–Calc. deviation (cm^{-1}); Δ_2, maximum Obs.–Calc. deviation (cm^{-1}); For $H_2{}^{17}O$ the estimated (see text) vibrational energy of (210) is marked by '*'.

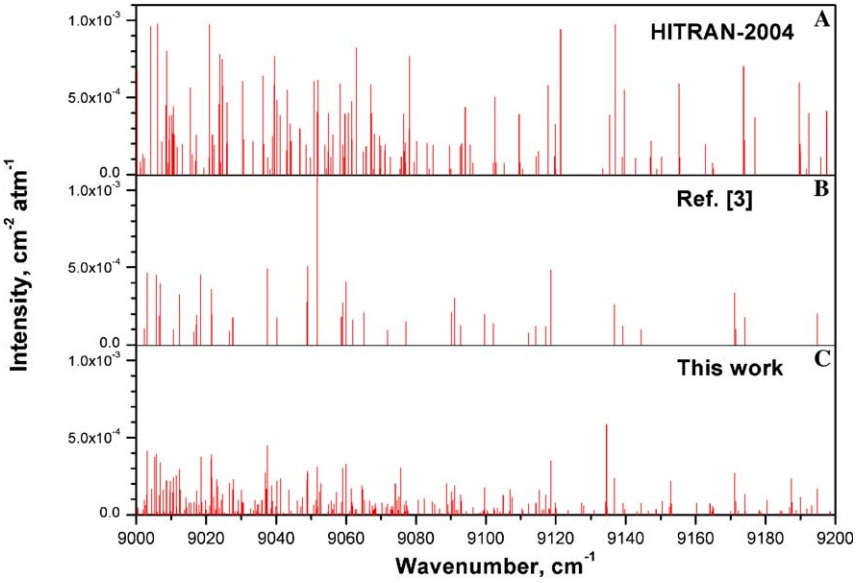

Fig. 4. Comparison of the pure $H_2{}^{17}O$ and $H_2{}^{18}O$ stick spectrum (at 296 K) in the 9000– 9200 cm^{-1} selected region: (A) HITRAN-2004 data; (B) Reference [3] data; (C) experimental data derived from this work. Absorption lines in this region correspond mainly to the (012)–(000) band.

theoretical intensity calculation [8] had definite drawbacks, in particular for line intensities of the (031)–(000) band, which were strongly underestimated.

The comparison with HITRAN-2004 has shown that the $H_2{}^{18}O$ and $H_2{}^{17}O$ lines included in this recent database may deviate from our precise positions by up to $-4.2\ cm^{-1}$ and $-3.3\ cm^{-1}$ for $H_2{}^{18}O$ and $H_2{}^{17}O$, respectively. The intensity comparison, however, is much better: the ratio of our intensities with respect to those of HITRAN-2004 is equal to 0.83 on average, though for some vibrational bands like (012)–(000) this ratio may be considerably less as seen in Fig. 4. Thus it is demonstrated that the most serious problems of HITRAN-2004 in the 8000–9500 cm^{-1} region concern not only, as stated in [3], the old experimental results [1,2] (where only natural water FT spectra were recorded and assigned), but also a large set (911 transitions) of $H_2{}^{18}O$ and $H_2{}^{17}O$ lines included in the HITRAN-2004 database, for which the spectroscopic parameters are not reliable.

4. Derivation of energy levels and evidence for local high-order resonances

The energy levels derived from the assigned transitions by adding ground state energy levels of [13] are given in Tables 2 and 3 for the $H_2{}^{18}O$ and $H_2{}^{17}O$ molecules, respectively. They are retrieved mainly from the Hefei spectra for $H_2{}^{18}O$ and from the Kitt Peak spectra for $H_2{}^{17}O$. However, a few energy levels were taken from alternate spectra recorded in this study (see Section 2) and are identified by asterisks in Tables 2 and 3. Overall 514 rotational energy levels of the $H_2{}^{18}O$ molecule and 244 levels of the $H_2{}^{17}O$ molecule were derived belonging to (031), (111), (130), (210), (012), (050), and (060) vibrational states (see also

Table 2
Rotational energy levels of $H_2{}^{18}O$ vibrational states (cm^{-1})

J	K_a	K_c	(111)			(031)			(130)			(210)			(012)		
			E	δ	N	E	δ	N	E	δ	N	E	δ	N	E	δ	N
0	0	0	8779.7190		1	8341.1078		1	8249.0357		1	8739.5258		1	8967.5651		1
1	0	1	8802.9097	0.4	2	8364.7008	0.9	2	8272.3938	0.7	2	8762.5693	0.7	2	8990.8712	0.1	2
1	1	1	8816.8561	0.6	2	8387.9210	0.4	2	8297.6695	0.4	2	8777.1255	0.9	2	9004.2736	0.1	3
1	1	0	8822.4565	0.3	2	8394.1251	0.1	2	8303.7772	0.1	2	8782.6832	0.5	2	9009.9370	0.4	2
2	0	2	8847.8619	0.8	4	8410.7558	0.2	3	8318.0914	0.2	2	8807.3213	0.6	2	9036.0064	0.3	3
2	1	2	8857.4743	0.3	4	8428.6629	0.4	3	8338.3209	0.6	4	8817.6515	1.1	3	9045.2391	0.7	3
2	1	1	8873.6818	0.4	3	8447.5338	0.4	3	8356.6105	0.5	3	8834.2771	0.5	2	9062.2043	1.2	2
2	2	1	8915.8652	0.5	3	8515.2854	0.1	2	8429.5499	0.2	3	8878.1964	0.3	4	9101.9721	0.2	3
2	2	0	8917.2387	0.2	3	8516.3689	0.6	2	8430.8294	0.3	2	8878.9293	0.6	2	9103.4216	0.5	2
3	0	3	8912.2616	0.1	3	8477.2714	0.1	2	8384.2820	0.2	3	8871.5692	0.0	2	9100.5835	0.6	2
3	1	3	8917.7389	0.5	5	8489.6904	0.2	2	8398.6801	0.4	3	8877.6877	0.5	3	9105.8287	0.3	2
3	1	2	8952.1403	0.3	4	8526.7233	0.8	3	8435.0463	0.1	3	8910.6265	0.6	3	9139.4225	0.6	3
3	2	2	8985.1924	0.1	5	8586.1730	0.4	3	8499.8014	0.5	3	8945.6277	0.6	3	9171.9575	0.1	3
3	2	1	8991.5264	0.5	5	8591.3403	0.3	2	8504.6243	0.5	4	8952.8304	0.4	3	9178.6144	0.9	4
3	3	1	9067.8624	0.7	3	8709.6588	0.3	2	8630.5029	1.4	2	9031.9194	0.6	2	9251.8008	0.3	2
3	3	0	9068.0860	0.0	2	8709.7850	0.4	2	8630.6047	0.8	4	9032.1002	0.2	2	9252.0445	0.1	2
4	0	4	8994.2568	0.3	4	8562.1514	0.4	3	8468.9606	0.0	2	8953.4420	0.1	2	9182.7869	1.7	2
4	1	4	8996.9290	0.3	3	8569.7531	0.2	2	8478.1658	0.1	3	8956.5610	0.5	2	9185.3345	0.6	4
4	1	3	9051.7094	0.4	5	8630.4893	0.7	4	8538.0041	0.8	3	9010.2555	0.6	2	9239.9129	0.9	2
4	2	3	9076.4635	0.6	5	8679.6732	0.7	4	8592.5581	0.4	5	9037.0969	0.3	3	9263.9828	0.2	4
4	2	2	9092.9921	0.6	6	8693.8509	0.2	3	8605.7048	0.6	3	9053.7223	1.6	3	9281.3004	0.7	3
4	3	2	9162.5525	0.4	3	8806.2654	0.2	3	8726.2102	0.4	6	9126.5754	0.4	5	9347.5571	0.1	2
4	3	1	9164.0389	0.3	5	8807.1102	0.8	3	8726.8884	0.7	3	9127.7660	0.4	2	9349.1665	0.5	3
4	4	1	9272.5418	0.0	2	8966.9087	0.2	2	8895.8506	1.1	3	9239.6107	0.2	2	9453.4465	0.6	3
4	4	0	9272.5663	0.3	3	8966.9242	0.0	2	8895.8612	2.1	2	9239.6453	0.3	2	9453.4799		1
5	0	5	9093.2687	0.2	3	8664.1332	0.7	2	8570.9604	0.1	3	9052.2551	0.7	3	9282.9180	0.2	4
5	1	5	9094.4213	0.6	4	8668.4039	0.4	3	8576.2104	1.0	2	9053.6948	1.0	2	9283.1871	0.2	2
5	1	4	9172.5305	0.9	6	8757.0766	0.3	2	8663.9063	1.2	4	9130.9967	0.5	3	9361.2435	0.5	4
5	2	4	9188.8141	0.4	5	8794.9905	0.2	2	8707.0910	0.4	3	9149.2786		1	9377.1049	0.7	3
5	2	3	9220.8923	0.4	5	8824.0742	0.3	3	8734.3137	0.2	3	9181.4721	0.6	3	9410.6998	0.5	3
5	3	3	9279.6118	0.6	4	8926.9345	0.5	3	8845.6245	1.9	4	9244.6019	1.8	2	9466.9421	0.1	2
5	3	2	9286.2591	0.6	4	8930.1143	0.0	2	8848.1326	0.5	3	9249.2334	0.2	2	9472.7327	0.2	3
5	4	2	9391.3754	0.4	5	9088.1498	0.0	3	9015.9328	6.9	2	9358.2068		1	9573.8092	3.1	2
5	4	1	9391.5820	0.8	2	9088.2326	0.9	3	9016.0065	1.0	2	9358.4769	1.2	2	9574.1022	0.1	2
5	5	1	9528.0023	0.6	3	9281.3148	0.3	4	9219.5841	1.7	2	9498.9834		1	9705.0704		1
5	5	0	9527.9988		1	9280.8976	0.3	4	9219.6016		1	9498.9960		1	9705.0721	0.2	3
6	0	6	9209.2759	0.6	4	8782.8866	1.1	3	8689.1416	0.0	2	9168.1292	1.9	2	9398.2657	3.1	2
6	1	6	9209.7937	0.4	3	8785.1692	0.1	2	8692.3505	0.1	2	9168.6753	0.6	2	9399.2147	0.6	3
6	1	5	9311.8944	0.1	3	8904.2622	0.7	3	8810.7191	2.1	3	9270.4016	0.8	2	9500.9902		1
6	2	5	9321.3098	0.6	4	8931.2584	0.3	4	8842.6019	0.8	4	9281.4373		1	9510.5220	0.3	4
6	2	4	9372.8930	0.5	6	8980.5394	0.3	3	8889.7063	0.3	2	9333.8257		1	9564.9396	0.1	2
6	3	4	9421.4828	0.5	3	9071.2327	0.6	3	8988.8478	0.3	2	9386.7900	0.5	3	9609.2311	0.4	3
6	3	3	9435.8804	0.1	4	9079.9205	0.3	3	8995.1586	2.6	4	9397.7587		1	9623.8933	1.8	2
6	4	3	9534.2547	0.6	4	9233.6752	0.0	2	9160.0182	2.7	2	9500.4194	0.8	3	9718.3410	0.6	3
6	4	2	9535.2834	0.1	3	9234.2265	0.5	4	9160.3195		1	9501.7523	1.4	2	9719.6757	0.1	2
6	5	2	9670.6084	1.2	2	9427.4880	1.7	4	9363.9365	1.2	3	9641.6573		1	9850.5553	0.6	3
6	5	1	9670.6136	0.3	2	9426.6122	0.4	3	9364.0692		1	9641.7746	0.7	2	9850.5989		1
6	6	1	9831.6243	2.2	2	9646.0464		1	9596.4079		1				0004.2977		1
6	6	0	9831.6268	0.7	2	9646.0459		1	9596.4042		1				0004.2940		1
7	0	7	9342.5760	0.2	2	8918.5216	0.1	2	8824.3769	0.6	2	9300.9268	1.0	2	9532.0849	1.1	2
7	1	7	9342.8175	0.1	3	8919.7240	0.1	2	8826.2567	1.4	2	9301.2559		1	9532.0687		1
7	1	6	9468.1132	0.4	4	9069.8335	1.1	2	8976.2918	1.1	3	9426.6972	1.5	2	9657.2247	0.2	2
7	2	6	9473.0389	0.4	4	9087.5908	0.7	3	8998.2903	2.2	2	9432.7323		1	9660.8855		1
7	2	5	9555.4483	0.0	2	9164.3476	0.1	3	9070.3533	0.1	2	9509.0803	2.7	2	9741.5285	0.9	2
7	3	5	9584.5445	0.4	4	9238.4707	0.3	4	9152.4097		1	9543.9856	0.8	4	9773.4411	0.2	2
7	3	4	9612.9816	1.0	4	9257.4809	0.5	2	9168.2820	0.2	3	9573.7647	1.1	2	9801.9232		1
7	4	4	9700.9271	0.7	3	9403.3184	0.5	2	9327.9690		1	9668.5499	0.7	2	9886.7479	1.8	2
7	4	3	9704.5113	0.9	3	9405.1456	0.8	2	9329.3765	0.1	2	9670.1705	1.2	2	9891.0864	1.3	2
7	5	3	9837.1972	0.3	2	9597.5350	0.5	6	9531.7002	5.6	2	9808.2013		1	10019.8711	2.5	3
7	5	2	9837.2979	0.7	3	9596.5650	1.5	3	9532.4079		1	9809.3656	3.1	3	10020.0971	0.7	4

Note. N is the number of lines used for the upper level determination and δ denotes the corresponding experimental uncertainties in 10^{-3} cm^{-1}. Energy level of $H_2{}^{18}O$ derived from the Kitt Peak's spectrum (see text) is marked by '*'.

Table 2 (*continued*)

J	K_a	K_c	(111)			(031)			(130)			(210)			(012)		
			E	δ	N	E	δ	N	E	δ	N	E	δ	N	E	δ	N
7	6	2	9997.6837	0.2	2	9816.3960	1.3	2				9974.7207		1	10170.6468		1
7	6	1	9997.6609		1	9816.3918		1				9974.7110		1	10170.6435	3.2	2
7	7	1	10187.3635	1.3	2	10055.4332		1	10021.5818		1	10165.5097		1	10348.7005		1
7	7	0	10187.3636	1.3	2	10055.4332		1	10021.5813		1	10165.5151		1	10348.7001		1
8	0	8	9493.2048	0.7	3	9071.2019	0.4	2	8976.5116		1	9451.1393		1	9682.9106		1
8	1	8	9493.3232	0.6	2	9071.5342	0.3	2	8977.7347	0.4	3	9451.3039		1	9683.0830		1
8	1	7	9640.7577	0.4	4	9252.2679		1	9158.9714	0.9	2	9599.6686		1	9830.1752	3.5	2
8	2	7	9643.2800	1.4	4	9263.1891	1.5	2	9173.4893	1.8	3	9602.4736	0.6	2	9832.5774	0.6	3
8	2	6	9748.8040	0.4	4	9368.5612	1.6	3	9274.2963		1	9704.9678		1	9937.6726		1
8	3	6	9768.6397	0.7	3	9427.7577		1	9339.9739	3.7	2	9731.8611	0.5	3	9958.5213	0.1	2
8	3	5	9815.9568	1.5	5	9462.8800	0.7	2				9776.2600		1	10009.7827		1
8	4	5	9890.8476	0.6	4	9596.3495		1				9857.4773	0.4	2	10078.4424	0.1	2
8	4	4	9900.3584	0.7	3	9601.6394	0.4	3							10089.4173		1
8	5	4	10027.7858	0.5	3	9791.5988		1	9721.9351		1	9998.4820		1	10212.9712	1.1	4
8	5	3	10028.2878	0.0	2	9790.6686	0.3	4							10213.8127		1
8	6	3	10187.7165	0.4	3	10010.6402		1				10165.1525	4.5	2	10361.1016	3.3	1
8	6	2	10187.6115	0.3	2	10010.6428	2.8	2									
8	7	2	10380.9685		1	10250.5797		1							10540.9497		1
8	7	1	10380.9685	0.1	3	10250.5795		1							10540.9443		1
8	8	1	10588.7135		1	10499.8528		1									
8	8	0	10588.7135		1	10499.8528		1									
9	0	9	9661.2204	0.5	3	9241.0412	0.0	2	9145.7120	1.6	2	9618.5247		1	9851.5113		1
9	1	9	9661.4651	0.5	2	9241.2883	0.2	2	9146.7476		1	9618.8017		1	9851.5826		1
9	1	8	9830.0502	0.3	2	9451.0145		1	9357.9694		1				10020.2969	2.5	2
9	2	8	9831.9610	0.5	3	9457.3969	0.3	2							10020.0066		1
9	2	7	9961.4673	0.6	2				9499.3110		1	9918.2415		1	10150.9864	1.9	2
9	3	7	9972.7597	0.4	2	9638.1106	0.6	4									
9	3	6	10044.1128	3.4	3							10002.8680		1	10238.6993		1
9	4	6	10103.2193	0.4	3	9812.9997	0.3	3				10070.0720		1			
9	4	5	10123.4960	3.8	3	9824.4594		1				10086.1995		1			
9	5	5	10242.1506	0.6	3	10009.4566	4.1	3	9943.5856		1						
9	5	4	10244.0134	2.3	2	10008.9030		1							10432.0508		1
9	6	4	10401.7064		1	10228.5066	3.0	2									
9	6	3	10401.4090		1	10228.5918		1									
9	7	3	10597.9462	1.7	2	10469.1756		1									
9	7	2				10469.1699		1									
9	8	2	10807.0964		1	10718.4253		1									
9	8	1	10807.0964		1	10718.4253		1									
10	0	10	9847.7510	0.1	3	9428.1094	2.4	2				9803.4073		1			
10	1	10	9845.9523	0.2	2	9428.1839	0.7	2	9333.5686		1	9803.8242		1	10037.4946*		1
10	1	9	10036.3436	0.8	2	9666.1650		1				9994.1700		1			
10	2	9	10035.1639	0.8	2	9669.7412		1				9996.4363		1	10226.2884		1
10	2	8	10191.0992	0.2	4	9840.0712	0.2	2									
10	3	8	10195.9442	0.6	2	9869.5411		1							10388.6815		1
10	3	7	10306.4730	1.6	2	9951.3896		1									
10	4	7	10337.1469	1.1	2	10054.7373		1				10290.4009	0.3	2			
10	4	6	10372.4401	0.9	3	10074.3674		1									
10	5	6	10479.7928		1				10180.6357	0.2	2						
10	5	5	10485.1258	0.1	2	10251.3724	0.4	2									
10	6	5	10639.5626		1												
10	6	4	10638.9873	0.9	3	10470.0699		1									
10	7	3	10838.0732		1	10710.9491		1									
11	0	11	10048.7729		1	9632.4586		1							10240.6469		1
11	1	11	10048.7879	0.0	2	9632.3964	0.1	2									
11	1	10	10260.6617	0.1	2							10217.2049		1			
11	2	10	10258.7989	0.7	3	9899.8857		1									
11	2	9	10433.5082		1												
11	3	9	10437.3635	2.8	2	10119.2856		1									
11	3	8	10568.7987		1												
11	4	8	10591.5904	0.7	2	10315.1547	1.9	2				10550.6275		1			
11	5	7	10739.9948		1												
11	5	6	10752.1555		1												
11	6	6	10900.9724		1												
12	0	12	10268.2181	0.7	2	9854.2721		1									

Table 2 (*continued*)

J	K_a	K_c	(111)			(031)			(130)			(210)			(012)		
			E	δ	N	E	δ	N	E	δ	N	E	δ	N	E	δ	N
12	1	12	10268.0091	0.2	2												
12	1	11	10497.6477	1.7	2	10147.0885		1									
12	2	11	10499.1563		1												
12	2	10	10695.9749		1												
12	3	10	10696.4263		1												
12	3	9	10852.6961		1												
12	4	9	10865.5871		1												
12	4	8	10949.0779		1												
12	5	8	11021.8901		1												
13	0	13	10505.2716		1												
13	1	13	10505.2758	1.2	2	10092.8928		1									
13	1	12	10755.8070		1												
13	2	12	10754.5100		1												
13	3	11	10972.7855		1												
13	4	10	11158.2653		1												
14	0	14	10759.3217		1												
14	1	14	10759.3226		1												
14	1	13	11030.3580		1												
15	0	15	11030.3626		1												
15	1	15	11030.3633		1												
			(050)														
5	4	1	8567.0539	2.9	2												
8	4	4	9077.3369		1												
9	5	5	9591.3716		1												
10	5	6	9832.7077	0.4	2												
			(060)														
5	1	5	9245.4613	0.3	2												

Table 1). The set of obtained energy levels was also compared with the one of [3]: 220 and 84 levels for $H_2{}^{18}O$ and $H_2{}^{17}O$ molecules, respectively (see also Table 1). We confirmed all but three levels of the $H_2{}^{17}O$ molecule reported in [3], while nine levels, including the origin of the (012)–(000) band at 8967.4832 cm^{-1} were found to be incorrect (our value is 8967.5651 cm^{-1}) for $H_2{}^{18}O$. A set of 31 energy levels has been reported for the (031) state of $H_2{}^{18}O$ and $H_2{}^{17}O$ in a recent study [14]. They were derived from very weak transitions in the 6130–6749 cm^{-1} spectral region recorded by the extremely sensitive CRDS technique for natural water. Our analysis does not confirm three energy levels of this set. Thus, in total, we have derived 164 and 298 new energy levels for the $H_2{}^{17}O$ and $H_2{}^{18}O$ molecules, respectively. Though our energy levels agree well with [3] (absolute averaged deviation is 0.0024 cm^{-1}), individual levels may deviate significantly (up to 0.015 cm^{-1}) from [3]. We thus decided to provide the complete set of energy levels derived from the present assignment work. Their values should be more accurate since, as a rule, they have been retrieved from several lines allowing a check of combination differences.

It is well known that the deviations of the calculated energy levels [8] from the observed ones have a rather smooth behavior: they slowly change as J and K_a increase, providing a good criteria for the assignment especially for single lines. This smooth behavior is most evident for the Obs.–Calc. values of levels with the same K_a rotational numbers. So the observed trend of the $K_a = 0$ energy level deviations was used to evaluate the origin of the (210)–(000) band of $H_2{}^{17}O$ at 8749.91 ± 0.03 cm^{-1}. In Table 1, it is also shown that the energy level predictions in [8] appear to be quite accurate, with the largest deviation from the experimental data not exceeding 0.19 cm^{-1}. At the same time, in Tables X and XI of [8] it was stated that the average deviation of calculated transition wavenumbers from the HITRAN-92 [15] database in the studied region varied from −0.64 cm^{-1} for the (111)–(000) band of $H_2{}^{17}O$ up to −3.65 cm^{-1} for the (031)–(000) band of $H_2{}^{18}O$. This was reflecting the poor quality of the corresponding HITRAN-92 data for $H_2{}^{18}O$ and $H_2{}^{17}O$ (which were then transferred into HITRAN-2004), but did not correspond to the actual accuracy of the theoretical calculation.

The resonance interactions between ro-vibrational levels of the second hexad of $H_2{}^{17}O$ and $H_2{}^{18}O$ are similar to those of the $H_2{}^{16}O$ molecule [1,2]. Some of the energy levels of both hexads are perturbed by levels of the highly excited bending states (050) and (060) (see Tables 2 and 3). Thus, a number of (050) energy levels of $H_2{}^{18}O$ were derived from lines borrowing their intensities via Fermi and Coriolis-type interactions with the (031) and (130) states. Likewise, the strong (050) 10_{56}–9_{09} $H_2{}^{17}O$ transition at 8950.713 cm^{-1} steals its intensity from the (111) 10_{010}–9_{09} resonance partner at 8945.5458 cm^{-1}. It is interesting to note that the same

Table 3
Rotational energy levels of $H_2{}^{17}O$ vibrational states (cm^{-1})

J	K_a	K_c	(111)			(012)			(210)			(031)		
			E	δ	N	E	δ	N	E	δ	N	E	δ	N
0	0	0	8792.5443		1	8982.8692		1				*8356.5313		1
1	0	1	8815.7545	0.2	2	9006.1954		1	8772.9704		1			
1	1	1	8829.8688	0.1	2	9019.7444	0.3	2				*8403.5824		1
1	1	0	8835.4547	0.0	2	9025.3958		1	8793.2636		1	*8409.7779		1
2	0	2	8860.7655	0.1	2	9051.3917	0.7	2				*8426.2457	7.6	2
2	1	2	8870.5157	0.3	3	9060.7656	0.3	2	8828.3017		1	*8445.0103		1
2	1	1	8886.2192	0.0	2	9077.6886	2.1	3				*8463.2279		1
2	2	1	8929.3877	0.5	3	9117.8866	0.8	4	8889.8602	0.8	3			
2	2	0	8930.7417	0.3	3	9119.3175	0.4	2	8890.1105		1	*8532.6860	2.6	2
3	0	3	8925.2870	0.1	2	9116.0888	0.5	2						
3	1	3	8930.8688	0.1	3	9121.4473	0.6	3	8888.4247		1	*8505.4366	6.7	2
3	1	2	8965.0545	0.3	2	9154.9697	0.6	3	8921.2799		1			
3	2	2	8998.7456	0.1	4	9187.9375	0.1	2	8957.0151	0.5	2	*8602.5490	1.5	3
3	2	1	9004.9940	0.2	2	9194.5220	0.6	3	8963.9899	0.7	2			
3	3	1	9082.2143	0.5	3	9268.4355		1	9044.0829		1	*8727.0129		1
3	3	0	9082.4329	0.1	2	9268.6766	1.0	2	9044.2465		1			
4	0	4	9007.4589	0.1	3	9198.4655	0.3	2	8964.2046		1	*8577.8934	1.7	2
4	1	4	9010.1996	0.8	3	9201.0892	1.3	2	8967.4343		1			
4	1	3	9064.8757	0.2	3	9255.5723		1				*8646.3262	1.4	2
4	2	3	9090.0839	0.8	3	9280.0684	1.2	4	9048.4160		1			
4	2	2	9106.4059	0.6	3	9297.2200		1				*8710.1476	1.6	2
4	3	2	9176.9216	0.7	4	9364.2649	0.5	2	9138.8170	0.8	3			
4	3	1	9178.3712	0.2	4	9365.8373	0.0	2	9139.9391		1			
4	4	1	9288.0333	0.2	2	9471.0681		1	9253.0748		1			
4	4	0	9288.0537	2.6	3	9471.1020		1						
5	0	5	9106.3939	0.1	2	9298.3655	1.2	4	9063.2495		1			
5	1	5	9107.8742	0.6	3	9299.1143	0.3	2	9064.7563		1	*8684.4547		1
5	1	4	9185.9102	0.0	2	9377.0960	0.7	3	9141.9062		1			
5	2	4	9202.5573	0.1	3	9393.3282	1.0	2				*8811.5577	2.1	2
5	2	3	9234.2192	0.3	3	9426.6692	1.2	3						
5	3	3	9294.5764	0.4	5	9483.7482		1	9257.2798	0.4	2			
5	3	2	9299.8240	1.7	3	9489.4091	0.3	2	9261.3852	0.5	2			
5	4	2	9406.8818	0.6	3	9591.5371		1				*9106.8935		1
5	4	1	9407.0722	0.9	3	9591.8174	0.8	2	9371.9933		1	9107.2626	0.6	2
5	5	1	9544.9168	0.3	2							9301.4159		1
5	5	0	9544.9129		1	9723.9264	1.1	2				9301.8318	1.5	2
6	0	6	9222.9386	0.2	2	9414.3616		1	9179.5200		1			
6	1	6	9223.4719	0.4	3	9415.3189	1.0	2				*8801.4042		1
6	1	5	9325.5689	0.2	4	9517.1606		1						
6	2	5	9335.2478	0.9	4	9526.8829	0.8	2	9293.0586		1			
6	2	4	9386.1248	0.6	3	9581.0228		1						
6	3	4	9436.2731	0.3	4	9626.1512	0.7	2	9399.6603	1.0	3			
6	3	3	9450.6120	0.2	4	9640.5230	1.1	2						
6	4	3	9549.7904	0.3	2	9736.1807	1.4	2	9514.1097		1			
6	4	2	9550.7569	0.3	4	9737.4655		1						
6	5	2	9687.5174		1	9869.6321	1.4	2				9447.5006		1
6	5	1	9687.5270		1	9869.6738		1				9446.3525	1.4	3
6	6	1	9850.2008		1	10024.6046		1	9824.9740		1			
6	6	0	9850.2003		1	10024.6011		1	9825.0101		1			
7	0	7	9356.5093		1	9548.4497		1						
7	1	7	9356.7629	0.4	2	9548.2114		1	9312.8144		1			
7	1	6	9482.1515	1.2	3	9673.6748		1	9438.3201		1			
7	2	6	9487.2435	0.5	3				9444.6131		1	*9104.5450		1
7	2	5	9569.2554	1.4	2	9757.8445		1						
7	3	5	9599.3574	1.9	4									
7	3	4	9627.3419	1.6	3									
7	4	4	9716.5126	0.2	3									
7	4	3	9719.9243	0.6	3	9908.8984	0.8	2						
7	5	3	9854.1266		1							9617.7A231		1
7	5	2	9854.2094	1.3	2	10039.3860		1						
7	6	2	10016.2132	0.4	2									
7	6	1	10016.2110	3.2	2									
7	7	1	10208.4619		1	10370.6726		1						

Table 3 (*continued*)

J	K_a	K_c	(111)			(012)			(210)			(031)		
			E	δ	N	E	δ	N	E	δ	N	E	δ	N
7	7	0	10208.4616		1	10370.6721		1						
8	0	8	9507.4409	0.7	2				9463.0110		1			
8	1	8	9507.5666	0.9	2	9699.7461		1	9463.1715		1			
8	1	7	9655.1953	1.7	2				9611.0492		1			
8	2	7	9657.8269	1.4	2	9849.3884	0.6	2						
8	2	6	9763.0938	1.2	3									
8	3	6	9783.5952		1				9737.8375		1			
8	3	5	9830.2278	0.1	3									
8	4	5	9906.5157		1	10096.5571		1	9871.5201		1			
8	4	4	9915.6450	0.0	2									
8	5	4	10044.7461	0.5	2	10232.4677		1						
8	5	3	10045.1807		1									
8	6	2	10206.1231	3.0	2									
8	7	2	10402.3326		1									
8	7	1	10402.3321		1									
9	0	9	9675.7964		1				9630.7474		1			
9	1	9	9676.0978	1.1	2									
9	1	8	9844.9033		1				9800.7626		1			
9	2	8	9847.1391	2.0	2									
9	2	7	9976.2661		1									
9	3	7	9987.9699	1.4	2							9656.1397		1
9	3	6	10058.4220		1									
9	4	6	10119.0230	1.7	2									
9	4	5	10138.6147		1									
9	5	5	10259.1713		1									
9	5	4	10260.8526		1									
9	6	4	10420.2441		1									
10	0	10	9863.6478		1									
10	1	10	9860.9429		1									
10	1	9	10051.6459	1.5	2									
10	2	9	10050.6830		1									
10	2	8	10206.7732		1									
10	3	8	10211.5093		1									
10	4	7	10353.1509		1				10304.5900		1			
10	4	6	10387.6128		1									
10	5	5	10501.8438		1									
10	6	5	10658.1751		1									
10	6	4	10657.5109		1									
11	0	11	10064.1752		1									
11	1	11	10064.1355		1									
11	1	10	10276.5986		1									
11	2	10	10274.5831		1									
11	2	9	10449.5938		1									
11	3	9	10453.3698		1									
11	4	8	10607.8914		1									
12	0	12	10283.9859		1									
12	1	12	10283.7440		1									
12	1	11	10513.9297		1									
12	2	11	10515.4069		1									
13	2	12	10771.0793		1									
						(130)			(050)			(060)		
						E	δ	N	E	δ	N	E	δ	N
6	5	2				9381.8005		1						
7	5	3				9549.3445		1						
8	5	4				9746.6103		1						
10	5	6				10198.2455		1	9858.8150		1			
6	1	6										9381.3462		1

Note. N is the number of lines used for the upper level determination and δ denotes the corresponding experimental uncertainties in 10^{-3}cm^{-1}. Energy levels derived from the Hefei's spectrum (see text) are marked by'∗'.

(050) [10 5 6] energy level for the $H_2{}^{16}O$ molecule was recently observed through 6 lines resulting from the resonance interaction with the (111)–(000) band in [16]. Another type of high-order local resonance interaction also caused considerable intensity transfer from the (210)–(000) band lines of $H_2{}^{18}O$ to weak resonance partners of the (060)–(000) band, which made it possible to observe 3 lines of the latter band involving the [515] energy level of the (060) state. Similarly, the (060) [616] energy level of $H_2{}^{17}O$ at 9381.3462 cm^{-1} was observable through a resonance with the (111) [624] level. This unusual type of resonance interaction was observed for the first time in [1,2] and was later explained [16] as resulting from the strong centrifugal distortion effect typical of the H_2O molecule and resulting in a crossing of rotational levels of the highly excited bending states with ro-vibrational levels not belonging to the same normal mode polyad.

5. Conclusion

The high-resolution FT absorption spectra of $H_2{}^{17}O$ and $H_2{}^{18}O$ were recorded and analyzed for the first time in the 8000–9400 cm^{-1} spectral region. This led to the determination of a large set of 164 and 298 new accurate energy levels for five vibrational states belonging to the second hexad of the $H_2{}^{17}O$ and $H_2{}^{18}O$ molecules. Strong perturbations of the (210), (111) vibrational states caused by high-order interactions with the large v_2 bending (050) and (060) states were evidenced. The recent extensive predictions of water vapor line positions using a potential function retrieved from ab initio calculations and experimental data [8,9] proved to be of high quality for the analysis of the $H_2{}^{17}O$ and $H_2{}^{18}O$ absorption spectra. According to our study, it can be stated that in the 8000–9400 cm^{-1} spectral region, the HITRAN-2004 database contains more than 900 "simulated" $H_2{}^{17}O$ and $H_2{}^{18}O$ absorption lines which may deviate in position by up to $-4.2\ cm^{-1}$ from precise experimental data. Clearly, the present work has improved and extended our knowledge of water vapor absorption in the near IR.

Acknowledgments

This work was jointly supported by the Natural Science Foundation of China (Grants 20473079, 10574124), by the Chinese Academy of Science, by the INTAS foundation (project 03-51-3394), and by a collaborative project between CNRS and RFBR (PICS Grant 05-05-22001). This work also forms part of an effort by a Task Group of the International Union of Pure and Applied Chemistry (IUPAC, Project No. 2004-035-1-100). B. Voronin acknowledges the financial support from EC program FP6, Marie Curie Incoming Fellowships, Grant WWLC008535. O. Naumenko also thanks support from the Foundation for Educational Development and Research of USTC-SIAS for a guest professorship.

Appendix A. Supplementary data

Supplementary data for this article are available on ScienceDirect (www.sciencedirect.com) and as part of the Ohio State University Molecular Spectroscopy Archives (http://msa.lib.ohio-state.edu/jmsa_hp.htm).

References

[1] J.-Y. Mandin, J.-P. Chevillard, J.-M. Flaud, C. Camy-Peyret, Can. J. Phys. 66 (1988) 997–1011.
[2] J.-Y. Mandin, J.-P. Chevillard, J.-M. Flaud, C. Camy-Peyret, J. Mol. Spectrosc. 132 (1988) 352–360.
[3] R.N. Tolchenov, J. Tennyson, J. Mol. Spectrosc. 231 (2005) 23–27.
[4] J.-P. Chevillard, J.-Y. Mandin, C. Camy-Peyret, J.-M. Flaud, Can. J. Phys. 64 (1986) 746–761.
[5] R.A. Toth, Appl. Opt. 33 (1994) 4868–4879.
[6] J.-P. Chevillard, J.-Y. Mandin, J.-M. Flaud, C. Camy-Peyret, Can. J. Phys. 65 (1987) 777–789.
[7] C. Camy-Peyret, J.-M. Flaud, J.-Y. Mandin, A. Bykov, O. Naumenko, L. Sinitsa, B. Voronin, J. Quant. Spectrosc. Radiat. Transf. 61 (1999) 795–812.
[8] H. Partridge, D.W. Schwenke, J. Chem. Phys. 106 (1997) 4618–4639.
[9] D.W. Schwenke, H. Partridge, J. Chem. Phys. 113 (2000) 6592–6597.
[10] R. Schermaul, J.W. Brault, A.A.D. Canas, R.C.M. Learner, O.L. Polyansky, N.F. Zobov, D. Belmiloud, J. Tennyson, J. Mol. Spectrosc. 211 (2002) 169–178.
[11] J.-P. Chevillard, J.-Y. Mandin, J.-M. Flaud, C. Camy-Peyret, Can. J. Phys. 63 (1985) 1112–1127.
[12] L.S. Rothman, D. Jacquemart, A. Barbe, D. Chris Benner, M. Birk, L.R. Brown, M.R. Carleer, C. Chackerian Jr., K. Chance, L.H. Coudert, V. Dana, V.M. Devi, J.-M. Flaud, R.R. Gamache, A. Goldman, J.-M. Hartmann, K.W. Jucks, A.G. Maki, J.-Y. Mandin, S.T. Massie, J. Orphal, A. Perrin, C.P. Rinsland, M.A.H. Smith, J. Tennyson, R.N. Tolchenov, R.A. Toth, J. Vander Auwera, P. Varanasi, G. Wagner, J. Quant. Spectrosc. Radiat. Transf. 96 (2005) 139–204.
[13] R.A. Toth, J. Opt. Soc. Am. B9 (1992) 462–482.
[14] P. Macko, D. Romanini, S.N. Mikhailenko, O.V. Naumenko, S. Kassi, A. Jenouvrier, Vl.G. Tyuterev, A. Campargue, J. Mol. Spectrosc. 227 (2004) 90–108.
[15] L.S. Rothman, R.R. Gamache, R.H. Tipping, C.P. Rinsland, M.A.H. Smith, D. Chris Benner, V. Malathy Devi, J.-M. Flaud, C. Camy-Peyret, A. Goldman, S.T. Massie, L.R. Brown, R.A. Toth, J. Quant. Spectrosc. Radiat. Transf. 48 (1992) 469–507.
[16] A. Bykov, O. Naumenko, L. Sinitsa, B. Voronin, J.-M. Flaud, C. Camy-Peyret, R. Lanquetin, J. Mol. Spectrosc. 205 (2001) 1–8.